energies

MDPI

Article

Study of the Pure Deuterium Fuel Burning Rate in Z-Pinch Devices with Magneto-Inertial Confinement

Olzhas Bayakhmetov * and Assylkhan Azamatov

Institute of Nuclear Physics, Almaty 050032, Kazakhstan; aaa180896@gmail.com
* Correspondence: bayakhmetov.o.s.92@gmail.com

Abstract: The burning rate of pure deuterium (D-D) fuel in Z-pinch devices with magneto-inertial confinement was studied in this paper. The system of particle and energy balance equations for D-D fuel burning with a mixed D-T-^{3}He fusion cycle (D-D, D-T, and D-^{3}He reactions) was solved numerically, taking into account the densities of all reacted and produced ions (protons, deuterium, tritium, helium-3, and alpha-particles). The obtained results indicate that effective D-D fusion in Z-pinch devices can be successfully achieved under conditions of a hot, dense plasma with an initial temperature of 31 keV or higher. The initial ion density of deuterium and electron density were equal due to quasi-neutrality condition of the plasma, with both reaching 10^{24} m^{-3}. Although the obtained results show that the burning rate of D-D fuel is approximately 2.3 times slower and its power density notably lower than that of D-T fuel, pure deuterium plasma can be considered as a promising alternative to well-studied deuterium–tritium plasma, with potential future applications in magneto-inertial fusion (MIF) facilities.

Keywords: nuclear fusion; deuterium; D-D fuel; Z-pinch; burning rate

check for updates

Citation: Bayakhmetov, O.; Azamatov, A. Study of the Pure Deuterium Fuel Burning Rate in Z-Pinch Devices with Magneto-Inertial Confinement. *Energies* **2024**, *17*, 5297. https://doi.org/10.3390/en17215297

Academic Editor: Dan Gabriel Cacuci

Received: 11 September 2024
Revised: 30 September 2024
Accepted: 22 October 2024
Published: 24 October 2024

Copyright: © 2024 by the authors. Licensee MDPI, Basel, Switzerland. This article is an open access article distributed under the terms and conditions of the Creative Commons Attribution (CC BY) license (https://creativecommons.org/licenses/by/4.0/).

1. Introduction

Controlled nuclear fusion has grown significantly in importance over the last few decades. Nuclear fusion is a clean and safe power source [1] with the great potential to become the world's long-term energy solution [2] in the near future. However, as is well-known, there are a number of challenges in successfully achieving controlled nuclear fusion, especially the requirement for a high initial plasma temperature of 100–350 million °C (depending on the fuel type) and an ultra-high particle density of 10^{31} m^{-3} for inertial confinement facilities and 10^{20} m^{-3} for magnetic confinement facilities [3]. To reach the required conditions in practice, different concepts of nuclear fusion machines are used, in particular, magnetic confinement devices, such as tokamaks and stellarators, and inertial confinement devices, such as laser-based systems and magnetized target fusion. A great example is the ITER (International Thermonuclear Experimental Reactor) [4] in Cadarache, France, which has recently become a significant experimental step between modern fusion research and future power plants [5]. Nevertheless, scientists and engineers believe that even if the ITER project is successful, it will still take decades before fusion energy becomes commercially viable. Thus, there is now a growing need for developing alternative designs of fusion machines.

In recent times, plasma installations with combined magnetic and inertial confinement advantages, known as magneto-inertial fusion (MIF) systems [6,7], have been actively developed as new alternatives to traditional fusion devices. The Z-pinch [8] has become one of the leading candidates for controlled nuclear fusion, because it has almost reached the performance levels of the current most effective fusion machines [9]. An excellent example of this is the Z Pulsed Power Facility [10–12] at the Sandia National Laboratory, where Magnetized Liner Inertial Fusion (MagLIF) experiments have been recently performed [13]. In these experiments, deuterium–deuterium (D-D) or deuterium–tritium (D-T) fusion

fuel in a Z-pinch device has been compressed by a magnetic field created by a strong unidirectional current [14] passing through a liner composed of high atomic number elements, such as tantalum or tungsten. Additionally, experiments conducted recently have provided evidence that the sheared-flow-stabilized (SFS) Z-pinch can meet the conditions required to achieve $Q = 1$ in both D-T and D-D plasmas [15]. Therefore, the Z-pinch has the potential in advancing fusion research by combining the main advantages of both magnetic and inertial confinement features.

In modern nuclear fusion devices, isotopes of hydrogen, such as deuterium and tritium, are generally used as the main candidates [16] for fuel. It is a well-known fact that deuterium is an abundant fusion fuel source. In contrast, unlike deuterium, tritium is unstable and has a short half-life of about 12.32 years [17], so it must be produced artificially, mainly in nuclear reactors. As stated in [18], tritium can be efficiently generated through the D-D start-up of the reactor with the subsequent use of neutrons produced during a D-T fusion reaction in a breeding blanket. Thus, considering the above, pure deuterium (D-D) fuel is a promising energy source that should be researched further both theoretically and experimentally.

The main purpose of this article is to apply and extend the numerical methods, as developed and well-described in previous works [7,19,20], to study the pure deuterium (D-D) fuel burning rate in Z-pinch devices with magneto-inertial confinement. In this paper, we consider the plasma in a hot, dense, quasi-neutral state, with equal initial deuterium and electron densities of 10^{24} cm^{-3} and equal initial ion and electron temperatures of 31 keV, achieved through fast laser ignition of the plasma in a Z-pinch facility. The calculation results showed that the minimum temperature required to achieve effective nuclear fusion of pure deuterium fuel at such the high density was 31 keV.

2. Methods

The scheme of D-D fuel burning in a Z-pinch device with fast laser ignition is shown in Figure 1. The pure deuterium fuel is contained in a metallic capsule (made of ^{9}Be or ^{6}Li) with an electron–photon converter, composed of a high atomic number element, on the left side, which is exposed to a strong electromagnetic field as a powerful mega-ampere discharge pulse passes along the Z axis of the capsule. An initial plasma temperature of 31 keV is reached through fast laser ignition (femtosecond laser pulse). This model scheme was thoroughly studied and developed in previous works [7,19,20].

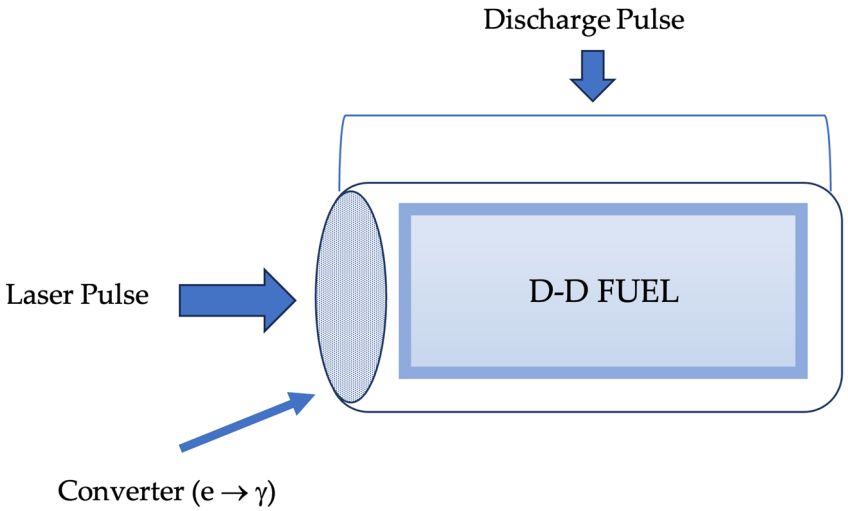


Figure 1. D-D fuel burning scheme in a Z-pinch device with fast laser ignition.

The main nuclear reaction used in the calculations is the deuterium–deuterium (D-D) fusion reaction, which has two channels of equal probability: $T + p$ and $^{3}He + n$. Meanwhile, it is worth noting that the D-T and D-^{3}He fusion reactions have the highest fusion

cross section and reaction rate [21,22] among other fusion reactions at low energies up to 1 MeV. Thus, taking this fact into account, these fusion reactions were also included in our calculations. Other fusion reactions were not considered, as they have a negligible probability at low energies compared to the reactions mentioned above. Finally, the full list of the nuclear fusion reactions used in this paper looks as follows:

$$D + D \rightarrow T(1.01) + p(3.02) + 4.03, \tag{1}$$

$$D + D \rightarrow {}^3He(0.82) + n(2.45) + 3.27, \tag{2}$$

$$D + T \rightarrow {}^4He(3.52) + n(14.07) + 17.59, \tag{3}$$

$$D + {}^3He \rightarrow {}^4He(3.67) + p(14.68) + 18.35. \tag{4}$$

where the numbers in brackets are the kinetic energies of ions, and the reaction energies are shown on the right side of the equations. All the values are expressed in units of MeV.

The burning rate of D-D fuel in Z-pinch devices with magneto-inertial confinement was obtained using a system of particle and energy balance differential equations. This system can be written as

$$\frac{dn_p}{dt} = \frac{1}{2}n_d^2\langle\sigma v\rangle_{DDp} + n_D n_{^3He}\langle\sigma v\rangle_{D^3He}, \tag{5}$$

$$\frac{dn_D}{dt} = -n_D^2\langle\sigma v\rangle_{DDp} - n_D^2\langle\sigma v\rangle_{DDn} - n_D n_T\langle\sigma v\rangle_{DT} - n_D n_{^3He}\langle\sigma v\rangle_{D^3He}, \tag{6}$$

$$\frac{dn_T}{dt} = \frac{1}{2}n_D^2\langle\sigma v\rangle_{DDp} - n_D n_T\langle\sigma v\rangle_{DT}, \tag{7}$$

$$\frac{dn_{^3He}}{dt} = \frac{1}{2}n_D^2\langle\sigma v\rangle_{DDn} - n_D n_{^3He}\langle\sigma v\rangle_{D^3He}, \tag{8}$$

$$\frac{dn_\alpha}{dt} = n_D n_T\langle\sigma v\rangle_{DT} + n_D n_{^3He}\langle\sigma v\rangle_{D^3He}, \tag{9}$$

$$\frac{dE_{tot}}{dt} = P_{ch} - P_{br}, \tag{10}$$

where n_p, n_D, n_T, $n_{^3He}$, and n_α are the densities of protons, deuterium (D), tritium (T), helium-3 (^{3}He), and alpha-particles, $\langle\sigma v\rangle_{mn}$ are the rates of fusion reactions corresponding to Equations (1)–(4), E_{tot} is the total energy density of the plasma in the capsule, P_{ch} is the fusion power density of charged particles (ions), and P_{br} is the power density of bremsstrahlung radiation. The capsule in a Z-pinch represents a closed cylinder, so there were no external sources and transport losses in the volume. In addition, synchrotron radiation was neglected because we considered the central hottest areas of the plasma, which were not affected by it. The reaction rates $\langle\sigma v\rangle_{mn}$ were considered as functions of the plasma temperature.

The total energy density is defined [20] as follows

$$E_{tot} = \frac{3}{2}\left[n_e\langle T_e\rangle + \sum_i n_i\langle T_i\rangle\right], \tag{11}$$

where n_e is the electron density, $\langle T_e\rangle$ and $\langle T_i\rangle$ are the average electron and ion temperatures. In Equation (11), the summation is taken over the densities of all ions from protons to alpha-particles. In addition, we assumed that all ions have the same temperature, equal to the average ion temperature $\langle T_i\rangle$. The electron density is defined through the quasi-neutrality condition [20] as follows

$$n_e = \sum_i Z_i n_i = n_p + n_D + n_T + 2n_{^3He} + 2n_\alpha, \tag{12}$$

The fusion power density of charged ions (in units of MeV/s/cm^3) is defined as

$$P_{ch} = \frac{1}{2}n_D^2\langle\sigma v\rangle_{DDp}Q_{DDp} + \frac{1}{2}n_D^2\langle\sigma v\rangle_{DDn}E_{^3He} + n_D n_T\langle\sigma v\rangle_{DT}E_{\alpha} + n_D n_{^3He}\langle\sigma v\rangle_{D^3He}Q_{D^3He}, \quad (13)$$

where the values of Q_{ij} are the reaction energies and the values of E_k are the kinetic energies of ions in units of MeV.

The fusion power density of neutrons (in units of MeV/s/cm^3) is obtained as follows

$$P_n = \frac{1}{2}n_D^2\langle\sigma v\rangle_{DDn}E_{n(DDn)} + n_D n_T\langle\sigma v\rangle_{DT}E_{n(DT)}, \quad (14)$$

where $E_{n(DDn)}$ and $E_{n(DT)}$ are the kinetic energies of neutrons (in units of MeV) corresponding to the fusion reactions given in Equations (2) and (3). Although this power density was not included in the calculations (neutrons escape outside the confinement vessel), it is important to obtain the ratio between charged ions and neutrons produced during the fusion processes in a Z-pinch device, because it generally helps to define the efficiency of nuclear fusion.

The power density of bremsstrahlung radiation (in units of MeV/s/cm^3) is defined as [23]

$$P_{br} = 0.334 \times 10^{-17} n_e T_e^{1/2} \sum_i n_i Z_i^2 \quad (15)$$

where T_e is the electron temperature in keV, n_e is the electron density in cm^{-3}, and n_i (in units of cm^{-3}) and Z_i are the ion density and charge number for each ion species.

The logarithmic reaction rates for the fusion reaction (1)–(4), averaged over the Maxwellian distribution, were obtained in [24] as follows

$$\lg\langle\sigma v\rangle(T) = \sum_{k=0}^{6}(\xi_k \cos kt + \eta_k \sin kt), \quad (16)$$

where t is defined as $t = \frac{\pi}{5.3}(\lg T - 3.65)$, and the temperature logarithm, $\lg T$, is in the range $1.0 \leq \lg T \leq 6.3$. The approximation coefficients, ξ_k and η_k, of the logarithmic reaction rates (16) are listed in Table 1.

Table 1. Approximation coefficients of $\lg\langle\sigma v\rangle(T)$ [24].

	D+D→T+p	***D+D→^{3}He+n***	***D+T→^{4}He+n***	***D+^{3}He→^{4}He+p***
ξ_0	−41.898	−42.145	−42.559	−60.504
η_0	0	0	0	0
ξ_1	30.017	30.484	33.312	53.039
η_1	24.313	24.459	24.394	43.244
ξ_2	−9.150	−9.451	−9.876	−16.233
η_2	−16.995	−17.170	−16.909	−31.497
ξ_3	2.140	2.265	2.501	3.980
η_3	7.572	7.744	7.406	15.707
ξ_4	−0.316	−0.346	−0.414	−0.749
η_4	−2.540	−2.655	−2.148	−6.055
ξ_5	0	0	0	0
η_5	0.580	0.630	0.411	1.734
ξ_6	0.012	0.015	0	0.004
η_6	−0.068	−0.079	0	−0.319

We employed the SciPy module [25] in the Python (3.8.18) programming language to solve the system of particle and energy balance Equations (5)–(10).

3. Results and Discussion

Figure 2 shows the pure deuterium (D-D) fuel burning rate over time in a Z-pinch device with magneto-inertial confinement. The total burning time reached approximately 6×10^{-8} s. The capsule initially contained only pure deuterium (D-D) fuel with a density of 10^{24} m^{-3}, and an initial plasma temperature of 31 keV due to ultrafast laser ignition. In recent work [20], the capsule contained deuterium–tritium (D-T) fuel with equal initial ion densities of 5×10^{23} m^{-3} for both deuterium and tritium. Thus, for a precise comparison with the results for D-T fuel, the full initial ion density of particles for D-D fuel was chosen as 10^{24} m^{-3}. However, it was proven in [7] that a starting plasma temperature of 10 keV is insufficient for effective D-D fuel burning in a hot, dense plasma, unlike in the case of D-T fuel. In contrast, our calculations showed that the minimum temperature for productive D-D fuel burning is in the range of 31 keV and above.

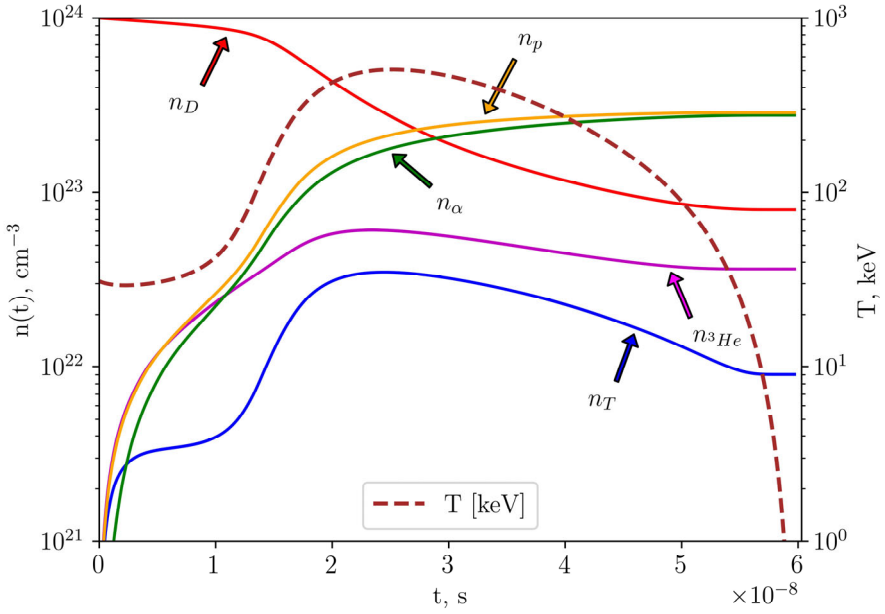


Figure 2. Change in ion densities and plasma temperature over time for D-D fuel.

The D-D fuel burning in the Z-pinch device started slowly despite the use of ultrafast laser ignition. The two D-D fusion reactions, corresponding to Equations (1) and (2), with the production of protons, tritium, and helium-3 ions, were dominant up to $t = 3 \times 10^{-9}$ s. As a result, the plasma temperature over this time slightly decreased and then remained nearly constant, not exceeding 31 keV. Tritium ions produced during the D-D fusion reaction in this period immediately began to fuse with deuterium ions up to $t = 1.2 \times 10^{-8}$ s. Consequently, from $t = 3 \times 10^{-9}$ s to $t = 1.2 \times 10^{-8}$ s, the tritium density was practically unchanged and the temperature remained almost the same, with a small gradient increase up to 40 keV. Over this time, the fuel burning process proceeded mainly due to D-D and D-T fusion. Simultaneously, the production of protons, helium-3 ions, and alpha-particles increased significantly, reaching nearly equal values with a slight dominance of protons. Starting from $t = 1.2 \times 10^{-8}$ s, the plasma temperature increased significantly, reaching a maximum of 508.342 keV by $t = 2.52 \times 10^{-8}$ s. During this period, the ion density of all produced particles rose significantly, leading to the rapid burning of deuterium. As a result, the density of deuterium decreased by approximately 73%. Finally, during the remaining period, the density of protons and alpha-particles grew gradually, achieving almost the same values at $t = 5.97 \times 10^{-8}$ s. In contrast, the D-^{3}He and D-T fusion reactions influenced

the process to a medium extent, leading to the moderate consumption of deuterium and ^{3}He ions.

Figure 3 shows the dependence of the power density of charged particles, bremsstrahlung radiation, and neutrons on time. After ultrafast laser ignition, the power density of charged ions achieved approximately 10^{31} MeV·cm^{-3}·s^{-1}, and then there was a gradual increase up to 2.57×10^{31} MeV·cm^{-3}·s^{-1} at $t = 7.16 \times 10^{-9}$ s. Subsequently, it grew significantly, reaching a maximum of 2.25×10^{32} MeV·cm^{-3}·s^{-1} at $t = 1.66 \times 10^{-8}$ s. After that, the power density of charged particles decreased rapidly to 1.53×10^{31} MeV·cm^{-3}·s^{-1} at $t = 4.9 \times 10^{-8}$ s, and finally dropped dramatically to below 10^{30} MeV·cm^{-3}·s^{-1} over the rest of the D-D fuel burning time.

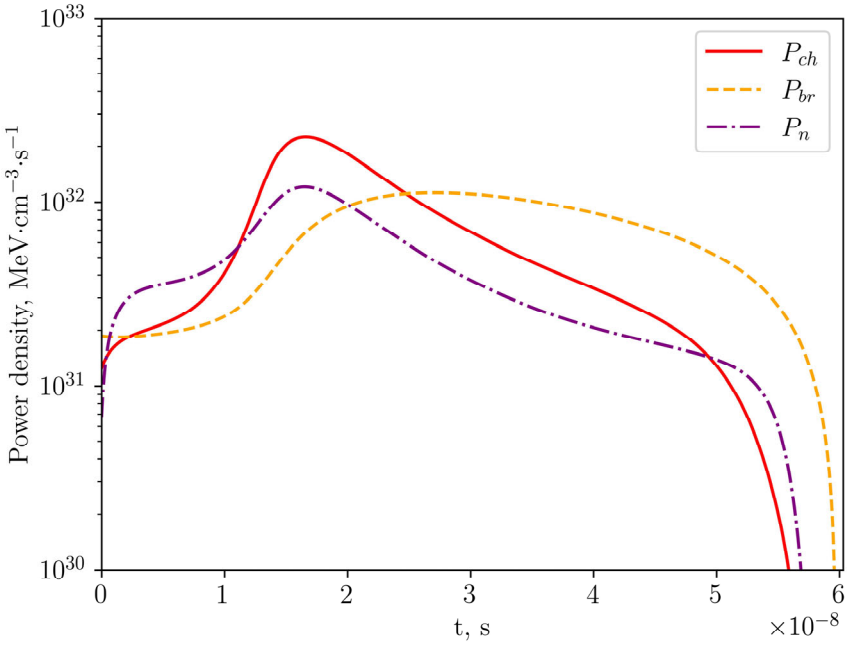


Figure 3. Power density of charged particles, bremsstrahlung radiation, and neutrons depending on time for D-D fuel.

After the D-D fuel ignition in the capsule, the power density of neutrons increased rapidly to 3.07×10^{31} MeV·cm^{-3}·s^{-1} at $t = 2.39 \times 10^{-9}$ s. From $t = 2.39 \times 10^{-9}$ s to $t = 6.57 \times 10^{-9}$ s it grew gradually to 3.77×10^{31} MeV·cm^{-3}·s^{-1}. Then, the power density of neutrons increased rapidly, reaching a peak of 1.21×10^{32} MeV·cm^{-3}·s^{-1} at $t = 1.66 \times 10^{-8}$ s. Figure 3 shows that the power density of neutrons exceeded those of charged ions from the ignition moment to $t = 1.2 \times 10^{-8}$ s. There was a rapid decrease to 1.32×10^{31} MeV·cm^{-3}·s^{-1} at $t = 5.07 \times 10^{-8}$ s, and eventually the power density of neutrons fell dramatically to below 10^{30} MeV·cm^{-3}·s^{-1} over the remaining time. From the obtained results, it can be concluded that, except for the period from ignition start to $t = 1.2 \times 10^{-8}$ s, the time dependence of the power density of charged ions and neutrons showed similar patterns.

Until $t = 6.57 \times 10^{-9}$ s, the power density of bremsstrahlung radiation remained nearly unchanged, not exceeding 2×10^{31} MeV·cm^{-3}·s^{-1}. Subsequently, it increased rapidly reaching a maximum of 1.12×10^{32} MeV·cm^{-3}·s^{-1} at $t = 2.71 \times 10^{-8}$ s. Then, the power density of bremsstrahlung radiation decreased gradually to 3.37×10^{31} MeV·cm^{-3}·s^{-1} at $t = 5.37 \times 10^{-8}$ s, and finally dropped dramatically to less than 10^{30} MeV·cm^{-3}·s^{-1} over the remaining period.

Figure 4 shows the time dependence of the energy density (in units of MeV/cm^3) of charged ions, neutrons, and bremsstrahlung radiation. The energy density of charged ions reached 1.3×10^{22} MeV/cm^3 at $t = 10^{-9}$ s, and increased to 2.65×10^{23} MeV/cm^3 at $t = 1.08 \times 10^{-8}$ s. Then, it grew gradually to 3.72×10^{24} MeV/cm^3 at $t = 5.97 \times 10^{-8}$ s.

The energy density of neutrons attained 1.34×10^{22} MeV/cm^3 at $t = 10^{-9}$ s, and increased gradually to 6.68×10^{23} MeV/cm^3 at $t = 1.46 \times 10^{-8}$ s, reaching the same value as the energy density of charged ions. Finally, it reached the value of 2.41×10^{24} MeV/cm^3 at $t = 5.97 \times 10^{-8}$ s. The energy density of bremsstrahlung radiation attained 1.66×10^{22} MeV/cm^3 at $t = 10^{-9}$ s. The energy density of bremsstrahlung radiation exceeded that of charged ions until $t = 6.5 \times 10^{-9}$ s, reaching 1.1×10^{23} MeV/cm^3. Eventually, it increased gradually reaching a maximum of 3.8×10^{24} MeV/cm^3 at $t = 5.97 \times 10^{-8}$ s. From the results presented in Figure 4, we can conclude that despite the use of ultrafast laser ignition for pure deuterium fuel burning, strong bremsstrahlung radiation, with energy comparable to that of charged particles fusion, leads to an insignificant change in temperature at the beginning of burning. As a result, a period of 6.5 nanoseconds is essential for the effective start of burning of pure deuterium (D-D) fuel in a Z-pinch device.

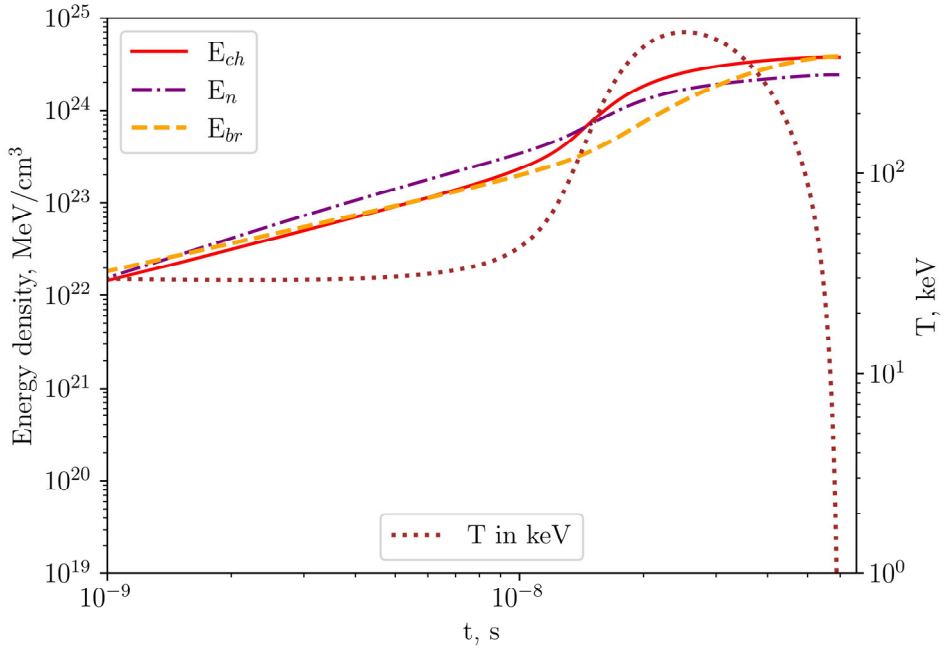


Figure 4. Energy density of charged ions, neutrons, and bremsstrahlung radiation.

Figure 5 shows the ratio between the energy of charged ions and the total fusion energy E_{ch}/E_{tot}. The total energy, E_{tot}, is the sum of the energies of charged ions, E_{ch}, and neutrons, E_n, and the ratio is determined as $\gamma = E_{ch}/(E_{ch} + E_n)$. Initially, at $t = 10^{-10}$ s, the ratio, γ, attained a value of 0.648, and decreased rapidly reaching a minimum of 0.39 at $t = 6.46 \times 10^{-9}$ s. Subsequently, it increased rapidly to 0.612 at $t = 3.55 \times 10^{-8}$ s. Until the end of D-D fuel burning, the ratio did not fall below the value of 0.60. As mentioned earlier, the effective burning of D-D fuel in a Z-pinch device starts at $t = 6.5 \times 10^{-9}$ s. As a result, this value corresponds to the minimum of the ratio between the energy of charged ions and the total fusion energy, or to the maximum of the ratio between the energy of neutrons and the total fusion energy, defined in [20] as $\delta = E_n/(E_{ch} + E_n)$. Thus, from the results presented in Figure 5, it can be concluded that effective D-D fuel burning requires a sufficient number of neutrons released in the D-D and D-T fusion reactions, given in Equations (2) and (3). Therefore, at low temperatures, pure deuterium fuel (D-D) burning in a Z-pinch device is mainly supported by the D-T fusion.

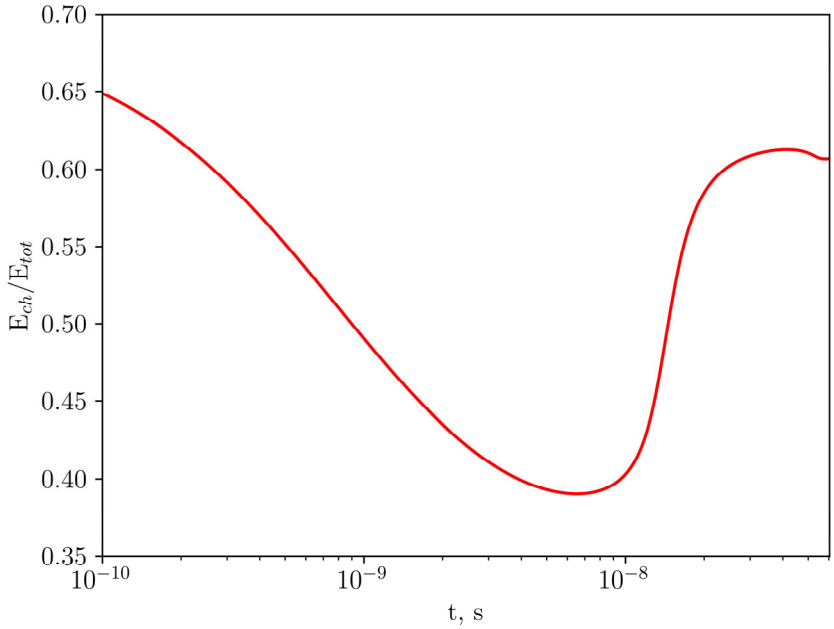


Figure 5. Ratio between charged ion energy and total fusion energy.

Since effective D-D fuel burning in a Z-pinch device was not achieved in previous work [7], it would be interesting to compare our results for pure deuterium (D-D) fuel with the results obtained for D-T fuel, using nearly identical initial burning conditions, except for the initial temperature. As described in [20], the capsule contained deuterium–tritium (D-T) fuel with initial ion densities of 5×10^{23} m^{-3} for both deuterium and tritium. Therefore, for D-D fuel, the full initial ion density of particles was chosen as 10^{24} m^{-3}. Thus, comparing this work's results with the results of theoretical study of the D-T fuel burning rate in Z-pinch devices with magneto-inertial confinement [20], the following conclusions can be drawn:

- The plasma temperature in the capsule with pure deuterium (D-D) fuel reached a peak of 508.342 keV at $t = 2.52 \times 10^{-8}$ s, whereas for deuterium–tritium (D-T) fuel in [20], it reached 300.38 keV at $t = 0.494 \times 10^{-8}$ s. Although the time dependence of temperatures for D-D and D-T fuel shows the same patterns, the burning rate of D-D fuel is notably slower than that of D-T fuel (almost 2.3 times slower!). Moreover, D-D fuel requires a higher initial temperature than D-T (31 keV compared to 10 keV). Nevertheless, unlike in [7], where the initial deuterium plasma temperature reached 10 keV, our results show that pure deuterium (D-D) plasma with an initial temperature of 31 keV or higher can be promising and effective in thermonuclear burning in magneto-inertial fusion (MIF) facilities.
- The fusion power density of charged ions for D-T fuel is higher than that for D-D fuel in a Z-pinch device. This can be seen from the results presented in Figure 6. The power density for D-T fuel reaches a maximum earlier and is approximately three times higher than that for D-D fuel—6.7×10^{32} MeV·cm^{-3}·s^{-1} at $t = 3.36 \times 10^{-10}$ s compared to 2.25×10^{32} MeV·cm^{-3}·s^{-1} at $t = 1.66 \times 10^{-8}$ s. The time dependence of the power density shows the same pattern for both D-T and D-D fuels. Although D-D fusion is less competitive than D-T fusion in terms of power density, and requires a higher initial plasma temperature, it can still be considered as a promising alternative to D-T fusion and a long-term energy solution in the future due to the abundant availability of deuterium.

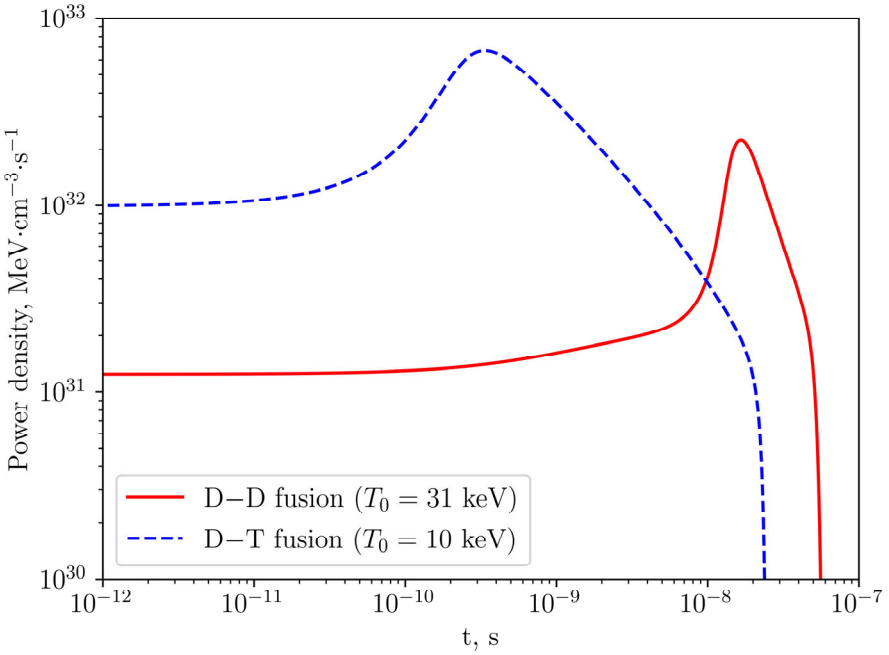


Figure 6. Fusion power density of charged ions for D-D and D-T fuel in a Z-pinch device.

4. Conclusions

The burning rate of pure deuterium (D-D) fuel in Z-pinch facilities with magneto-inertial confinement was considered in this work. As in the previous study [20], we numerically solved the system of particle and energy balance equations for pure deuterium fuel burning with a mixed D-T-^{3}He fusion cycle, taking into account the densities of all reacted and produced ions (protons, deuterium, tritium, helium-3, and alpha-particles).

The results of this paper show that effective D-D fusion in Z-pinch devices can be successfully achieved under conditions of a hot, dense plasma with an initial temperature of 31 keV or higher. Although the burning rate of D-D fuel is almost 2.3 times slower and the power density notably lower than that of D-T fuel, pure deuterium plasma can be considered as a promising alternative to well-studied deuterium–tritium plasma with future applications in magneto-inertial fusion facilities.

In conclusion, future investigations of the D-D fuel burning rate with more precise parameters, such as non-equal ion and electron temperatures, are required. Nevertheless, the results obtained in this paper can be further used for theoretical and experimental studies.

Author Contributions: Conceptualization, O.B.; methodology, O.B.; formal analysis, O.B.; investigation, O.B. and A.A.; resources, O.B. and A.A.; writing—original draft preparation, O.B.; writing—review and editing, O.B.; visualization, O.B. and A.A.; supervision, O.B.; project administration, O.B.; funding acquisition, O.B. All authors have read and agreed to the published version of the manuscript.

Funding: This research was funded by the Science Committee of the Ministry of Education and Science of the Republic of Kazakhstan (Grant No. AP14871936).

Data Availability Statement: Data are contained within the article.

Conflicts of Interest: The authors declare no conflicts of interest.

References

1. Rehm, T.E. Advanced Nuclear Energy: The Safest and Most Renewable Clean Energy. *Curr. Opin. Chem. Eng.* **2023**, *39*, 100878. [CrossRef]
2. Nicholas, T.E.G.; Davis, T.P.; Federici, F.; Leland, J.; Patel, B.S.; Vincent, C.; Ward, S.H. Re-Examining the Role of Nuclear Fusion in a Renewables-Based Energy Mix. *Energy Policy* **2021**, *149*, 112043. [CrossRef]
3. Meschini, S.; Laviano, F.; Ledda, F.; Pettinari, D.; Testoni, R.; Torsello, D.; Panella, B. Review of Commercial Nuclear Fusion Projects. *Front. Energy Res.* **2023**, *11*, 1157394. [CrossRef]

4. Juarez, R.; Pedroche, G.; Loughlin, M.; Pampin, R.; Martinez, P.; Pietri, M.; Alguacil, J.; Ogando, F.; Sauvan, P.; Lopez-Revelles, A.; et al. A Full and Heterogeneous Model of the ITER Tokamak for Comprehensive Nuclear Analyses. *Nat. Energy* **2021**, *6*, 150–157. [CrossRef]
5. Hassanein, A.; Sizyuk, V. Potential Design Problems for ITER Fusion Device. *Sci. Rep.* **2021**, *11*, 2069. [CrossRef]
6. Ryzhkov, S.V. Magneto-Inertial Fusion and Powerful Plasma Installations (A Review). *Appl. Sci.* **2023**, *13*, 6658. [CrossRef]
7. Seksembayev, Z.; Kukulin, V.; Sakhiyev, S. Study of a Dense Hot Plasma's Burning in Z-Pinch Devices with Inertial-Magnetic Confinement. *Phys. Scr.* **2018**, *93*, 085602. [CrossRef]
8. Haines, M.G. A Review of the Dense Z-Pinch. *Plasma Phys. Control Fusion* **2011**, *53*, 093001. [CrossRef]
9. Shumlak, U. Z-Pinch Fusion. *J. Appl. Phys.* **2020**, *127*, 200901. [CrossRef]
10. Sinars, D.B.; Sweeney, M.A.; Alexander, C.S.; Ampleford, D.J.; Ao, T.; Apruzese, J.P.; Aragon, C.; Armstrong, D.J.; Austin, K.N.; Awe, T.J.; et al. Review of Pulsed Power-Driven High Energy Density Physics Research on Z at Sandia. *Phys. Plasmas* **2020**, *27*, 070501. [CrossRef]
11. Ao, T.; Schollmeier, M.; Kalita, P.; Gard, P.D.; Smith, I.C.; Shores, J.E.; Speas, C.S.; Seagle, C.T. A Spherical Crystal Diffraction Imager for Sandia's Z Pulsed Power Facility. *Rev. Sci. Instrum.* **2020**, *91*, 043106. [CrossRef] [PubMed]
12. Savage, M.E.; Bennett, L.F.; Bliss, D.E.; Clark, W.T.; Coats, R.S.; Elizondo, J.M.; LeChien, K.R.; Harjes, H.C.; Lehr, J.M.; Maenchen, J.E.; et al. An Overview of Pulse Compression and Power Flow in the Upgraded Z Pulsed Power Driver. In Proceedings of the 2007 16th IEEE International Pulsed Power Conference, Albuquerque, NM, USA, 17–22 June 2007; Volume 2, pp. 979–984.
13. Ruskov, E.; Ney, P.; Rahman, H.U. The Staged Z-Pinch as a Potential Fusion Energy Source. *Phys. Plasmas* **2020**, *27*, 042709. [CrossRef]
14. Thompson, M.C.; Levitt, B.; Nelson, B.A.; Shumlak, U. Engineering Paradigms for Sheared-Flow-Stabilized Z-Pinch Fusion Energy. *Fusion Sci. Technol.* **2023**, *79*, 1051–1058. [CrossRef]
15. Shumlak, U.; Meier, E.T.; Levitt, B.J. Fusion Gain and Triple Product for the Sheared-Flow-Stabilized Z Pinch. *Fusion Sci. Technol.* **2024**, *80*, 1–16. [CrossRef]
16. De Temmerman, G. The Helium Bubble: Prospects for 3He-Fuelled Nuclear Fusion. *Joule* **2021**, *5*, 1312–1315. [CrossRef]
17. Abdou, M.; Riva, M.; Ying, A.; Day, C.; Loarte, A.; Baylor, L.R.; Humrickhouse, P.; Fuerst, T.F.; Cho, S. Physics and Technology Considerations for the Deuterium–Tritium Fuel Cycle and Conditions for Tritium Fuel Self Sufficiency. *Nucl. Fusion* **2020**, *61*, 013001. [CrossRef]
18. Pearson, R.J.; Antoniazzi, A.B.; Nuttall, W.J. Tritium Supply and Use: A Key Issue for the Development of Nuclear Fusion Energy. *Fusion Eng. Des.* **2018**, *136*, 1140–1148. [CrossRef]
19. Voronchev, V.T.; Kukulin, V.I. Implementation of the Thermonuclear Process in D3He-9Be Plasma on the Basis of a Z Pinch with an Ultrafast Laser Ignition. *Phys. Atom. Nucl.* **2010**, *73*, 38–58. [CrossRef]
20. Bayakhmetov, O.; Azamatov, A. Theoretical Study of the D-T Fuel Burning Rate in Z-Pinch Facilities with Magneto-Inertial Confinement. *Energies* **2024**, *17*, 3069. [CrossRef]
21. Jeet, J.; Zylstra, A.B.; Rubery, M.; Kim, Y.; Meaney, K.D.; Forrest, C.; Glebov, V.; Horsfield, C.J.; McEvoy, A.M.; Herrmann, H.W. Inertial-Confinement Fusion-Plasma-Based Cross-Calibration of the Deuterium-Tritium γ-to-Neutron Branching Ratio. *Phys. Rev. C* **2021**, *104*, 054611. [CrossRef]
22. Hosseinimotlagh, S.N. The Stopping Power of Relativistic Electrons and Laser-Accelerated Proton Beams for Fast Ignition of DT and D3He and P11B Fuels. *Int. J. Hydrogen Energy* **2016**, *41*, 1775–1790. [CrossRef]
23. Moreau, D.C. Potentiality of the Proton-Boron Fuel for Controlled Thermonuclear Fusion. *Nucl. Fusion* **1977**, *17*, 13. [CrossRef]
24. Belov, A.A.; Kalitkin, N.N.; Kozlitin, I.A. Refinement of Thermonuclear Reaction Rates. *Fusion Eng. Des.* **2019**, *141*, 51–58. [CrossRef]
25. Oliphant, T.E. Python for Scientific Computing. *Comput. Sci. Eng.* **2007**, *9*, 10–20. [CrossRef]

Disclaimer/Publisher's Note: The statements, opinions and data contained in all publications are solely those of the individual author(s) and contributor(s) and not of MDPI and/or the editor(s). MDPI and/or the editor(s) disclaim responsibility for any injury to people or property resulting from any ideas, methods, instructions or products referred to in the content.